Acta Biomaterialia 99 (2019) 320–329

Contents lists available at ScienceDirect

Acta Biomaterialia

journal homepage: www.elsevier.com/locate/actabiomat

Full length article

Zwitterion-functionalized dendrimer-entrapped gold nanoparticles for serum-enhanced gene delivery to inhibit cancer cell metastasis

Zhijuan Xiong [a], Carla S. Alves [b], Jianhua Wang [c,d], Aijun Li [a], Jinyuan Liu [a], Mingwu Shen [a], João Rodrigues [b], Helena Tomás [b], Xiangyang Shi [a,b,*]

[a] State Key Laboratory for Modification of Chemical Fibers and Polymer Materials, International Joint Laboratory for Advanced Fiber and Low-dimension Materials, College of Chemistry, Chemical Engineering and Biotechnology, Donghua University, Shanghai 201620, People's Republic of China
[b] CQM-Centro de Química da Madeira, Universidade da Madeira, Campus da Penteada, 9000-390 Funchal, Portugal
[c] Cancer Institute, Fudan University Shanghai Cancer Center, Fudan University, Shanghai 200032, People's Republic of China
[d] School of Medicine, Anhui University of Science & Technology, Huainan 232001, People's Republic of China

ARTICLE INFO

Article history:
Received 25 June 2019
Received in revised form 5 September 2019
Accepted 5 September 2019
Available online 9 September 2019

Keywords:
HIC1 gene
Dendrimers
Zwitterions
Gold nanoparticles
Gene delivery

ABSTRACT

We demonstrate a novel serum-enhanced gene delivery approach using zwitterion-functionalized dendrimer-entrapped gold nanoparticles (Au DENPs) as a non-viral vector for inhibition of cancer cell metastasis *in vitro*. Poly(amidoamine) dendrimers of generation 5 decorated with zwitterion carboxybetaine acrylamide (CBAA) and lysosome-targeting agent morpholine (Mor) were utilized to entrap gold NPs. We show that both Mor-modified and Mor-free Au DENPs are cytocompatible and can effectively deliver plasmid DNA encoding different reporter genes to cancer cells in medium with or without serum. Strikingly, due to the antifouling property exerted by the attached zwitterion CBAA, the gene delivery efficiency of Mor-modified Au DENPs and the Mor-free Au DENPs in the serum-containing medium are 1.4 and 1.7 times higher than the corresponding vector in serum-free medium, respectively. In addition, the Mor-free vector has a better gene expression efficiency than the Mor-modified one although the Mor modification enables the polyplexes to have enhanced cancer cell uptake. Wound healing and hypermethylated in cancer 1 (HIC1) protein expression assay data reveal that the expression of HIC1 gene in cancer cells enables effective inhibition of cell migration. Our findings suggest that the created zwitterion-functionalized Au DENPs may be employed as a powerful vector for serum-enhanced gene therapy of different diseases.

Statement of Significance

One major challenge in the non-viral gene delivery system is that the strong interaction between serum protein and the positively charged vector/gene polyplexes neutralize the positive charge of the polyplexes and form possible protein corona, thereby significantly reducing their cellular uptake efficiency and subsequent gene transfection outcome. Here we demonstrate the conceptual advances in the serum-enhanced gene delivery using zwitterionic modification of polycationic poly(amidoamine) (PAMAM) dendrimer-entrapped gold nanoparticles (Au DENPs). We demonstrate that partial zwitterionic modification of Au DENPs is able to confer them with antifouling property to resist serum protein adsorption. Hence the vector/DNA polyplexes are able to maintain their positive potentials and small hydrodynamic size in the serum environment, where serum solely play the role as a nutrition factor for enhanced gene delivery. We demonstrate that partial modification of zwitterion carboxybetaine acrylamide (CBAA) and morpholine (Mor) onto the surface Au DENPs renders the vector with both antifouling property and lysosome targeting ability, respectively. The generated functional Au DENPs can compact pDNA to form polyplexes that enable serum-enhanced gene expression. In particular, once complexed with hypermethylated in cancer 1 (HIC1) gene, the polyplexes can significantly inhibit cancer cell migration and metastasis.

* Corresponding author.
E-mail address: xshi@dhu.edu.cn (X. Shi).

https://doi.org/10.1016/j.actbio.2019.09.005
1742-7061/

1. Introduction

Gene therapy has gained much attention for its ability in correcting or compensating some genetic disorders by delivery of exogenous therapeutic genes to disease site [1–3]. These exogenous genes usually include some special DNA fragment embedded in plasmid and small interfering RNA (siRNA), such as B-cell lymphoma/leukemia-2 (Bcl-2) siRNA, which has the ability to knockdown the expression of the Bcl-2 protein. Recently hypermethylated in cancer 1 (HIC1) gene has been considered as a candidate tumor suppressor gene [4]. Studies have shown that in most of the common human cancer types, HIC1 is usually epigenetically silenced [4], such as in renal cell carcinoma [5], hepatocellular carcinoma [6,7], pancreatic cancer [8], prostate cancers [9,10] and hyperparathyroid tumors [11], etc. The metastasis of cancer is generally associated with the methylation of HIC1 promoter [12]. For instance, the metastasis of squamous cell carcinoma can be impaired via the HIC1 expression by demethylation [13]. Therefore, demethylation of HIC1 or transfection of demethylated HIC1 gene to cancer cells to express HIC1 protein can be considered as a powerful approach to inhibit the cancer cell metastasis.

High gene delivery efficiency usually relies on the selection of appropriate gene delivery vectors, including viral and non-viral vector systems [14]. However, the application of viral vector system was hampered due to the safety concerns, such as immunogenicity [15–18]. Hence, non-viral vectors are getting increasing attention because of their non-immunogenicity, high gene compaction capacity, and low cytotoxicity [19,20]. Poly(amidoamine) (PAMAM) dendrimers have been proven to be one of the non-viral vectors with excellent gene delivery efficiency due to their typical structural characteristics including monodispersity, well-defined three-dimensional molecular geometry, tailored surface functionalities, and availability from commercial resources [21,22]. The abundant terminal amines of PAMAM dendrimers endow them with strong ability to condense gene and to deliver the gene to cells. Studies have shown that PAMAM dendrimers can escape from lysosomes by proton sponge effect originating from their tertiary amines to protect gene from degrading by various enzymes in the lysosome [23].

Previously, we designed generation 5 (G5) PAMAM dendrimer-entrapped gold nanoparticles (Au DENPs) as a powerful vector for improved gene delivery performance [24]. The enhanced gene delivery efficiency relies on the fact that the entrapped Au core NPs preserve the 3-dimensional spherical shape of the dendrimers for better condensation of plasmid DNA (pDNA) and compensate part of the dendrimer terminal amines to alleviate their cytotoxicity. In another work, Au DENPs modified with arginine-glycine-aspartic peptide were shown to be capable of compacting pDNA carrying the human bone morphogenetic protein-2 gene for highly effective and specific stem cell gene delivery to induce osteogenic differentiation [25]. The same Au DENPs can also compact Bcl-2 or vascular endothelial growth factor siRNA for specific silencing of the expression the corresponding proteins for gene therapy of glioblastoma cells [22].

Normally, to realize improved gene delivery *in vitro*, the transfection medium needs to exclude the presence of serum, because the serum protein strongly interacts with the positively charged vector/gene polyplexes, resulting in low cellular uptake and consequently low gene delivery efficiency [26]. In another way, cells will lack sufficient nutritional support in the serum-free environment, and hence having difficulty to remain healthy [27,28]. Therefore, it would be ideal to develop a novel protein-resistant vector system to keep the formed positively charged vector/gene polyplexes to be intact in a serum culture environment for highly efficient gene delivery.

Earlier studies have shown that Au NPs modified with polyethylene glycol (PEG) display good antifouling properties for effective computed tomography (CT) imaging applications [29]. In a recent study, we demonstrate that NPs such as iron oxide NPs [30] or manganese oxide NPs [31] can be modified with zwitterions with equal molar positive and negative charges in close neighborhood to be rendered with better antifouling property for enhanced tumor magnetic resonance imaging than the corresponding particles modified with PEG. Very recently, Wang et al. modified G5 PAMAM dendrimers with carboxybetaine acrylamide (CBAA) to afford the dendrimers with outstanding compatibility with protein and cells [32]. Particularly, the CBAA-modified dendrimers could well keep their architecture and size in aqueous solution in the presence of fibrinogen, and their hydrodynamic size did not show appreciable changes. In our previous study, we have shown that CBAA-decorated Au DENPs display a better antifouling property, much less macrophage cellular uptake and liver accumulation, and longer blood circulation time than the PEGylated counterpart material, thereby allowing for improved lymph node, blood pool, and tumor CT imaging [33]. Therefore, it is quite logic to speculate that Au DENPs partially functionalized with zwitterionic materials may be developed as a novel gene vector that can resist serum adsorption for enhanced gene delivery applications.

In the present study, we illustrate the synthesis and application of zwitterion and morpholine (Mor)-functionalized Au DENPs for serum-enhanced HIC1 gene delivery to inhibit cancer cell metastasis (Fig. 1). The modification of Mor, which is a lysosome targeting ligand [34], is to check if the vector/pDNA polyplexes have better cellular uptake and hence better gene delivery performance than the Mor-free Au DENPs. CBAA and Mor-PEG-COOH were first synthesized and covalently decorated onto the surface of G5 PAMAM dendrimers. Then the G5 dendrimers were utilized to entrap Au NPs to get the product of $\{(Au^0)_{25}$-G5.NH_2-PEG-Mor$\}$ NPs. As a control, the $\{(Au^0)_{25}$-G5.NH_2-CBAA-*m*PEG$\}$ NPs were also synthesized. The two materials were systematically characterized, and their gene delivery efficacy was evaluated in a serum-free and serum environment, respectively. The influence of Mor on the lysosome escape of Au DENPs/pDNA polyplexes was tested by intracellular trafficking and localization assay. Finally, the serum-enhanced HIC1 gene delivery was confirmed by testing the inhibition ability of cancer cell metastasis via wound healing and Western blot assays. To our knowledge via a thorough literature investigation, our study supplies the very first example associated with the development of serum-enhanced gene delivery method using zwitterion-functionalized Au DENPs for inhibition of cancer cell metastasis.

2. Materials and methods

2.1. Synthesis of Au DENPs

Synthesis of HOOC-PEG-Mor: (R)-Morpholine-3-carboxylic acid hydrochloride (Mor-COOH, 41.90 mg, 0.25 mmol) was firstly dissolved into water (10 mL), and activated by 1-ethyl-3-(3-dimethylaminopropyl) carbodiimide hydrochloride (EDC, 47.93 mg, in 5 mL water) and N-hydroxysuccinimide (NHS, 28.85 mg, in 5 mL water) under strong magnetic stirring for 3.5 h. The activated Mor-COOH was then dropwise added into the water solution of HOOC-PEG-NH_2 (100.00 mg, 10 mL) while stirring for 3 days at room temperature. Then the mixture was thoroughly dialyzed against phosphate buffered saline (PBS, 3 times, 4 L) and water (3 times, 4 L) using a 500–1000 molecular weight cut-off (MWCO) membrane for 3 days, and finally lyophilized to get the product of HOOC-PEG-Mor.

Synthesis of G5.NH_2-CBAA-*m*PEG and G5.NH_2-CBAA-PEG-Mor: G5.NH_2-CBAA was synthesized according to the literature [33]. Mor-PEG-COOH (16.93 mg, in 7.8 mL water) was firstly activated by EDC (7.83 mg, in 5 mL water) and NHS (4.71 mg, in 2 mL water) under vigorous magnetic stirring for 3.5 h, then dropwise added into the G5.NH_2-CBAA solution (25.00 mg, in 10 mL water) under stirring for 3 days at room temperature. Then the mixture solution was extensively dialyzed against PBS (3 times, 4 L) and water (3 times, 4 L) through an 8000–14000 MWCO membrane for 3 days, and then lyophilized to get the product of G5.NH_2-CBAA-PEG-Mor. The G5.NH_2-CBAA-*m*PEG was synthesized under the same conditions described above.

Synthesis of {$(Au^0)_{25}$-G5.NH_2-CBAA-*m*PEG} and {$(Au^0)_{25}$-G5.NH_2-PEG-Mor} NPs: G5.NH_2-CBAA-PEG-Mor (30.00 mg, in 5 mL water) or G5.NH_2-CBAA-*m*PEG (30.59 mg, in 5 mL water) was mixed with $HAuCl_4{\cdot}4H_2O$ (4.38 mg, in 0.133 mL water) under strong magnetic stirring for 30 min. Then, $NaBH_4$ (2.01 mg, in 1 mL water) was rapidly injected to the above mixture solution while stirring for 3 h at room temperature. At last, the mixture solution was subjected to the same dialysis and lyophilization processes to get the product of {$(Au^0)_{25}$-G5.NH_2-CBAA-*m*PEG} or {$(Au^0)_{25}$-G5.NH_2-PEG-Mor} NPs.

2.2. Preparation and characterization of vector/pDNA polyplexes

The vector/pDNA ({$(Au^0)_{25}$-G5.NH_2-CBAA-*m*PEG}/pDNA or {$(Au^0)_{25}$-G5.NH_2-PEG-Mor}/ pDNA) polyplexes were prepared at N/P ratios (the molar ratio of primary amines of the dendrimers to phosphates in the pDNA backbone) of 0.25:1, 0.5:1, 1:1, 2:1, 4:1 and 8:1, respectively. We used three types of pDNAs encoding enhanced green fluorescent protein (EGFP), Luciferase (Luc), or HIC1 to prepare the polyplexes. Keeping the constant pDNA amount at 1 μg, both vector and pDNA solutions were diluted with PBS (pH = 7.4) to 50 μL and then mixed together to reach a final volume of 100 μL for each polyplex. The polyplex solutions were gently vortexed and room temperature incubated for 15 min. By varying the vector concentrations, polyplexes having different N/P ratios were obtained. To measure the hydrodynamic size and surface potential of the vector/pDNA polyplexes, pDNA (5 μg) dissolved in PBS was condensed by {$(Au^0)_{25}$-G5.NH_2-CBAA-*m*PEG} or {$(Au^0)_{25}$-G5.NH_2-PEG-Mor} in PBS to attain an eventual volume of 1 mL at an N/P ratio of 0.25, 0.5, 1, 2, 4 or 8. The prepared Au DENPs/pDNA polyplexes were characterized by gel retardation assay, dynamic light scattering (DLS), zeta-potential measurements, and transmission electron microscopy (TEM) according to literature protocols [23]. See additional experimental details in Supporting Information.

2.3. Statistical analysis

One-way ANOVA statistical analysis was performed to evaluate the significance of the experimental data. A p value of 0.05 was selected as the significance level, and the data were indicated with (*) for $p < 0.05$, (**) for $p < 0.01$, and (***) for $p < 0.001$, respectively.

3. Results and discussion

3.1. Synthesis and characterization of functional Au DENPs

Zwitterion modification has been proven to render materials with antifouling property and protein resistance ability [31,35]. In this work, we attempted to improve the gene delivery efficiency of Au DENPs *via* zwitterion modification of the dendrimer surface to exclude the serum protein adsorption and to solely use the serum nutrition for enhanced gene transfection of cells. First, CBAA was synthesized according to the literature [33] and was conjugated with G5.NH_2 dendrimers through Michael addition to generate the G5.NH_2-CBAA conjugates. Mor with carboxyl group was reacted with NH_2-PEG-COOH *via* EDC coupling to get the Mor-PEG-COOH segments, which were then connected with the G5.NH_2-CBAA conjugates through EDC chemistry. The thus created G5.NH_2-CBAA-PEG-Mor dendrimers were employed as templates to entrap Au NPs to get the final product of {$(Au^0)_{25}$-G5.NH_2-CBAA-PEG-Mor} NPs (Fig. 1). As a control, the Mor-free NPs of {$(Au^0)_{25}$-G5.NH_2-CBAA-*m*PEG} were also

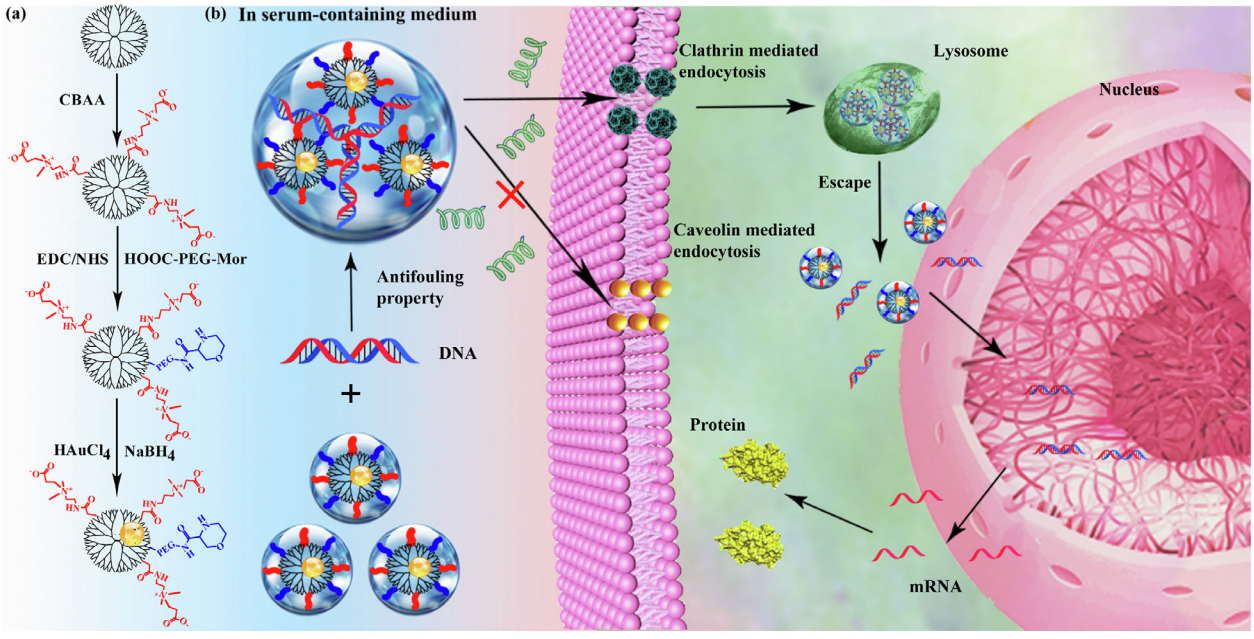

Fig. 1. Schematic illustration of the synthesis procedure of {$(Au^0)_{25}$-G5-CBAA-PEG-Mor} DENPs (a) for gene delivery applications (b). Notes for abbreviation: generation 5 (G5), carboxybetaine acrylamide (CBAA), polyethylene glycol-morpholine (PEG-Mor), dendrimer-entrapped nanoparticles (DENPs), 1-ethyl-3-(3-dimethylaminopropyl) carbodiimide hydrochloride (EDC), N-hydroxysuccinimide (NHS), and PEG-Mor with the other end of carboxyl group (COOH-PEG-Mor).

synthesized. The intermediate materials and final product were fully characterized using different techniques.

^{1}H NMR spectral characterization was used to characterize the structure of the generated Mor-PEG-COOH segments, G5.NH$_2$-CBAA dendrimers, {(Au^0)$_{25}$-G5.NH$_2$-CBAA-PEG-Mor} NPs, and {(Au^0)$_{25}$-G5.NH$_2$-CBAA-*m*PEG} NPs (Fig. S1). The peak at 6.325 ppm assigned to the amide bond suggests the successful connection of PEG and Mor, and through NMR peak integration each PEG has been attached with 0.6 Mor (Fig. S1a). The proton peak at 1.86 ppm can be attributed to the –NHCH$_2$CH$_2$CH$_2$N$^+$- methylene protons of CBAA, and by comparison of the NMR integration of the G5 dendrimer and CBAA methylene protons [33], the number of CBAA connected with each G5 dendrimer was estimated to be 17.9 (Fig. S1b). The –CH$_2$- protons of PEG at 3.5–3.8 ppm were also used to compare with the G5 dendrimer methylene protons. There are 16.8 Mor-PEG-COOH and 15.3 *m*PEG coupled to each G5 dendrimer for the G5.NH$_2$-CBAA-PEG-Mor and G5.NH$_2$-CBAA-*m*PEG conjugate, respectively (Fig. S1c-d).

The synthesized functional G5 dendrimers were employed to entrap Au NPs. Previously, we have shown that at the G5 dendrimer/Au salt molar ratio of 1: 25, the gene delivery efficiency of Au DENPs was optimal [24]. Hence, we used the same dendrimer/Au salt molar ratio to synthesize the {(Au^0)$_{25}$-G5.NH$_2$-CBAA-PEG-Mor} and {(Au^0)$_{25}$-G5.NH$_2$-CBAA-*m*PEG} NPs. The final products were characterized by UV–vis spectrometry (Fig. S2) and TEM (Fig. 2a and c). The surface plasmon resonance (SPR) band absorption showing at around 512 nm implies the formation of Au NPs. The mean diameter of Au core sizes was measured to be 1.5 nm and 1.6 nm for {(Au^0)$_{25}$-G5.NH$_2$-CBAA-PEG-Mor} and {(Au^0)$_{50}$-G5.NH$_2$-CBAA-*m*PEG} NPs, respectively. These results suggest that the different modifications of PEG-Mor and *m*PEG do not appreciably affect the formation of Au core NPs. In both cases, the Au core NPs display good crystallinity, and the lattices of Au crystals can be easily observed in the high-resolution TEM images (insets of Fig. 2a and c). Furthermore, we measured the gold content for each type of Au DENPs quantitatively by inductively coupled plasma-optical emission spectroscopy, and the data show that the added Au salt has been completely reduced to create the Au NPs.

For effective condensation of pDNA, we measured the mean number of primary amines of the Au DENPs by Primary Amino Nitrogen (PANOPA) assay kit (Table S1). The prepared {(Au^0)$_{25}$-G5.NH$_2$-CBAA-PEG-Mor} and {(Au^0)$_{25}$-G5.NH$_2$-CBAA-*m*PEG} NPs possess 50 and 53 primary amines per dendrimer on their surface, respectively, which are smaller than that of the pristine G5.NH$_2$ dendrimers reported in our prior study [36]. The actual residual primary amines of {(Au^0)$_{25}$-G5.NH$_2$-CBAA-PEG-Mor} and {(Au^0)$_{25}$-G5.NH$_2$-CBAA-*m*PEG} NPs are less than those

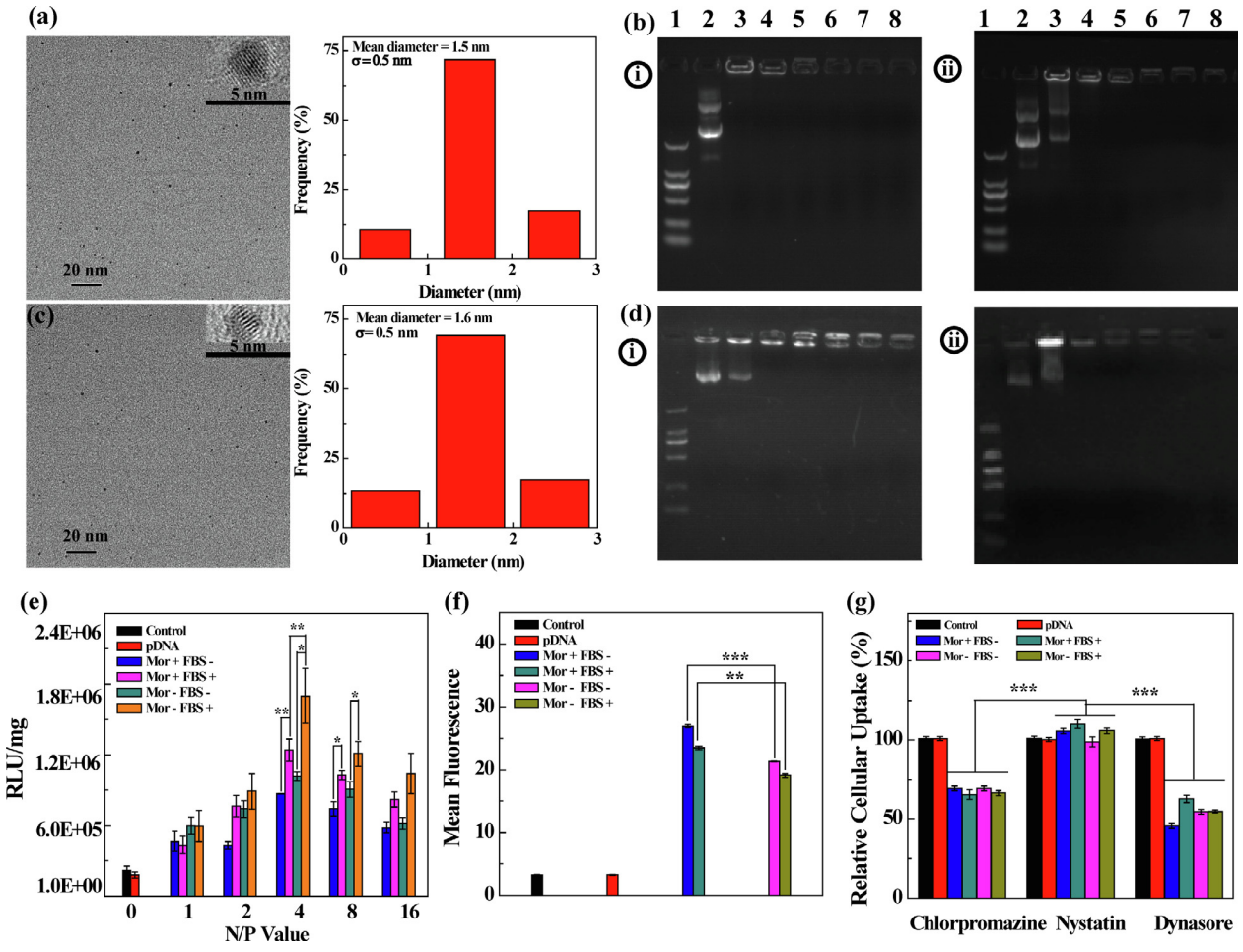

Fig. 2. TEM images and size-distribution histograms of {(Au^0)$_{25}$-G5.NH$_2$-CBAA-PEG-Mor} (a) {(Au^0)$_{25}$-G5.NH$_2$-CBAA-*m*PEG} (c) NPs. Agarose gel retardation assay of vector/pEGFP DNA (b) and vector/pHIC1 DNA (d) polyplexes at various N/P ratios ({(Au^0)$_{25}$-G5.NH$_2$-CBAA-PEG-Mor} (i) and {(Au^0)$_{25}$-G5.NH$_2$-CBAA-*m*PEG} (ii)). Lane 1: DNA marker; lane 2: pDNA alone; lane 3: N/P = 0.25:1; lane 4: N/P = 0.5:1; lane 5: N/P = 1:1; lane 6: N/P = 2:1; lane 7: N/P = 4:1; and lane 8: N/P = 8:1. (e) Luc gene transfection efficiency in HeLa cells using polyplexes at N/P ratios of 1, 2, 4, 8, and 16, respectively. (f) Flow cytometry analysis of HeLa cells treated with vector/Cy3-labeled pEGFP DNA polyplexes at an N/P ratio of 4 (5×10^4 cell/well seeding density, 3 h incubation with polyplexes in FBS-free or FBS-containing medium). (g) Uptake of Cy3-labeled pEGFP DNA in cells that were first incubated with endocytic pathway inhibitors before transfection using the pEGFP DNA polyplexes at an N/P ratio of 4 under the conditions of (f).

in theory, likely because part of dendrimer primary amines has been compensated for stabilizing the internal Au core NPs.

CBAA was used to modify PAMAM dendrimers to render the vector with a good antifouling property. The protein resistance ability of the vector was evaluated by testing the interaction between Au DENPs and bovine serum albumin (BSA) according to the literature [33]. The absorption of the Au DENPs/BSA mixture was measured at 278 nm *via* UV–vis spectrometry (Fig. S4) at the time of mixing BSA and Au DENPs and after 4 h incubation, followed by centrifugation. Then the change on the absorbance value (Δ absorbance) was quantified. The absorbance of the mixture increases with the concentration of Au DENPs; however, the Δ absorbance barely changes. Meanwhile, the absorbance and Δ absorbance show no appreciable differences between BSA/Mor-modified Au DENPs and BSA/Mor-free Au DENPs mixtures. These data indicate that the CBAA modification renders the vector with good protein-resistance property regardless of the positive surface potentials of the vectors. The good antifouling property of Au DENPs is expected to afford the subsequent vector/pDNA polyplexes with the same property for enhanced gene delivery applications.

3.2. Characterization of vector/pDNA polyplexes

The ability of vectors to compact pDNA was first evaluated by agarose gel retardation assay under different N/P ratios (Fig. 2b and d). Obviously, at a higher N/P, the migration of the pDNA can be more effectively retarded. At the N/P value of 0.5 or above, the migration of two kinds of pDNAs can be efficiently inhibited by both {$(Au^0)_{25}$-G5.NH_2-CBAA-PEG-Mor} and {$(Au^0)_{25}$-G5.NH_2-CBAA-*m*PEG} NPs. This implies that both vectors regardless of the modification of PEG-Mor or *m*PEG can compact pDNA. We then selected vector/pDNA polyplexes with an N/P ratio of 0.5 or above for the following *in vitro* assays.

The surface potential and hydrodynamic size of vector/pDNA polyplexes were measured. As shown in Figs. S3a and S3c, the vectors of {$(Au^0)_{25}$-G5.NH_2-CBAA-PEG-Mor} and {$(Au^0)_{25}$-G5.NH_2-CBAA-*m*PEG} NPs are positively charged. At a low N/P ratio, both vectors are unable to condense the pDNA, similar to the gel retardation assay data. With the increase of N/P value, the surface potential of the Au DENPs/pDNA polyplexes increases and levels off at around +30 mV at an N/P ratio of 2 or above. The hydrodynamic sizes of the polyplexes at an N/P ratio of 0.5 or above are in the range of 100–400 nm. Particularly, at an N/P ratio of 4, the polyplexes for both pEGFP and pHIC1 DNAs are quite small in hydrodynamic size. The positive surface potential and the small hydrodynamic size of the Au DENPs/pDNA polyplexes ensure their subsequent effective cellular uptake for gene transfection applications [37].

3.3. Cytotoxicity assay

Before the transfection of vector/pDNA polyplexes to HeLa cells, the cytotoxicity assay of vector and vector/pDNA polyplexes was carried out (Fig. S5). Clearly, in the studied dendrimer concentration range (0–3000 nM), both vector and vector/pDNA polyplexes show low cytotoxicity to HeLa cells. At the highest concentration of 3000 nM, the cell viability can still reach above 80%. There is no significant difference between cells treated with {$(Au^0)_{25}$-G5.NH_2-CBAA-PEG-Mor} and {$(Au^0)_{25}$-G5.NH_2-CBAA-*m*PEG} NPs under the same dendrimer concentrations. It should be noted that the cytotoxicity of pristine G5.NH_2 dendrimers is quite high due to the abundant dendrimer terminal amines [24], and the surface modification of CBAA and PEG-Mor or *m*PEG and internal entrapment of Au core NPs largely compromise their amine-induced cytotoxicity, which is essential for safe gene delivery applications.

3.4. Expression of EGFP and Luc genes

pDNA encoding EGFP or Luc genes was condensed by Au DENP vectors for transfection of HeLa cells. The EGFP gene transfection assay was utilized to qualitatively assess the ability of transfection efficiency of vector/pDNA polyplexes in serum-containing (FBS+) or serum-free (FBS−) environment. As shown in Fig. 3, the green fluorescence signal of cells is the strongest at the N/P of 4:1 for all experimental groups compared to other groups at the N/P ratios of 1:1, 2:1, 8:1 and 16:1, respectively. Interestingly, the groups with FBS show more EGFP gene expression than those without FBS. In general, the serum-containing medium often leads to protein adsorption onto the cationic polyplexes, resulting in low gene transfection efficiency [38,39]. In most of the *in-vitro* gene delivery studies, the transfection process needs to exclude the presence of serum to improve the gene transfection efficiency. Our data suggest that in the FBS-containing medium, the polyplexes are not interfered due to the antifouling property of the vectors afforded by CBAA modification [33], instead the FBS solely plays the role of nutrition to cell culture for serum-enhanced gene delivery. We next checked the role of Mor modification played on the gene transfection efficiency. Clearly, the Mor modification does not seem to significantly improve the gene delivery efficiency of the vectors, as the green fluorescence signal in the Mor + groups is lower than that in the Mor – groups at most of the studied N/P ratios. This may be due to the fact that with the Mor modification, more polyplexes are able to enter the lysosome of cells, and the lyosomal escape of the polyplexes may be hindered, which compromises the gene expression in cell nuclei to some extent.

Luc gene expression assay was also conducted to quantitatively assess the gene transfection efficiency (Fig. 2e). The results nearly coincide with those of the EGFP gene transfection data. The best Luc expression appears at the N/P ratio of 4 for all polyplexes transfected with or without FBS. At the N/P ratio of 4, the Luc expression in HeLa cells treated with Mor-free {$(Au^0)_{25}$-G5.NH_2-CBAA-*m*PEG}/pDNA polyplexes is significantly higher than that treated with Mor-modified polyplexes under the same conditions ($p < 0.01$). Meanwhile, the average light unit for the Luc expression in HeLa cells transfected in the serum-containing medium is 1.43 and 1.66 times higher than that in HeLa cells transfected in serum-free medium for Mor-modified polyplexes and Mor-free polyplexes, respectively at the N/P ratio of 4. This further illustrates the serum-enhancing effect of gene transfection, and supports that the Mor-modification does not seem to improve the gene delivery efficacy.

3.5. Cellular uptake of Au DENPs/pDNA polyplexes

In order to investigate the differences of cellular uptake of polyplexes with or without Mor modification, the pEGFP DNA labeled with Cy3 was complexed with the respective Au DENPs at an N/P ratio of 4 and the cells were incubated for 3 h before flow cytometry assay (Fig. 2f). To our surprise, the cellular uptake of Mor-modified polyplexes is significantly higher than that of Mor-free polyplexes regardless of the presence and absence of FBS in the transfection medium ($p < 0.01$). In contrast, there is nearly no difference between the mean fluorescence of HeLa cells treated with serum-containing or serum-free medium under the same transfection conditions ($p > 0.05$). This suggests that the decoration of CBAA onto the vector surface is able to efficiently reduce the adsorption of protein to polyplexes, and the presence of FBS does not seem to impact the cellular uptake efficiency of the polyplexes.

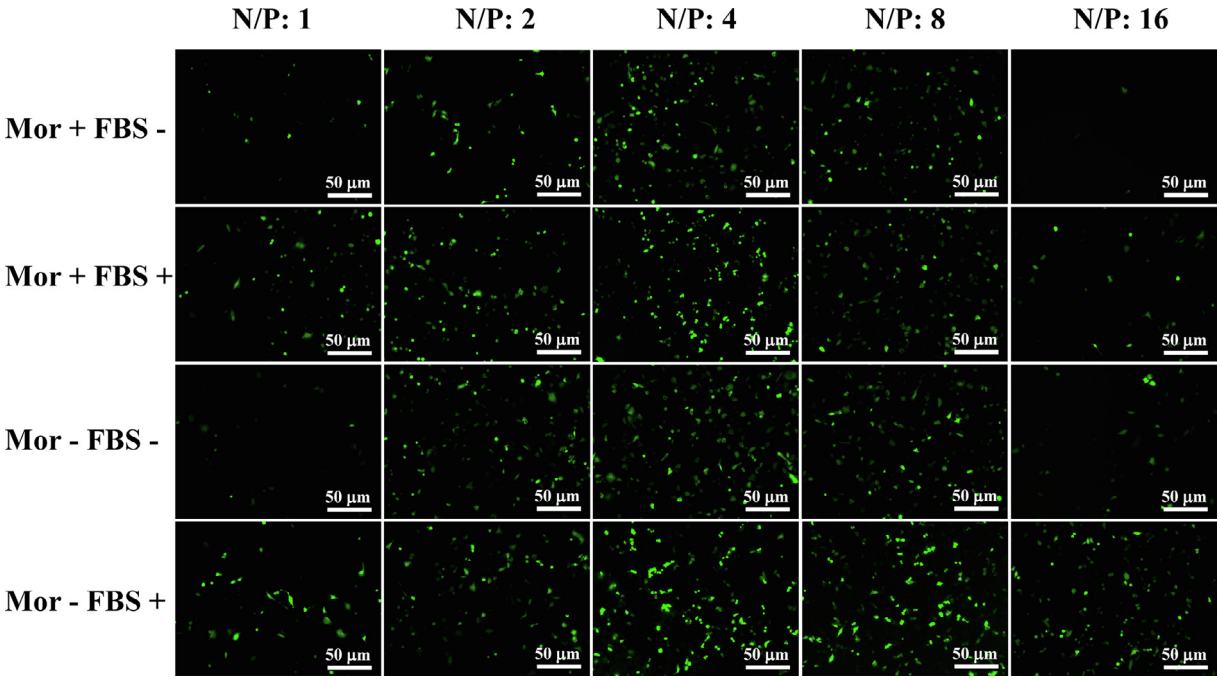

Fig. 3. Fluorescence microscopic images of EGFP gene expression in HeLa cells after transfection for 24 h by {$(Au^0)_{25}$-G5-CBAA-PEG-Mor}/pEGFP DNA polyplexes in FBS-free medium (Mor + FBS −) and FBS-containing medium (Mor + FBS +), and {$(Au^0)_{25}$-G5-CBAA-*m*PEG}/pEGFP DNA polyplexes in FBS-free medium (Mor − FBS −) and FBS-containing medium (Mor − FBS +), respectively.

3.6. Impacts of endocytic pathway inhibitors on the cellular uptake of the polyplexes

To further explore the cellular uptake pathway of the vector/pDNA polyplexes, HeLa cells were first treated with endocytic pathway inhibitors of chlorpromazine, dynasore and nystatin, respectively, followed by transfection of the polyplexes. The clathrin-mediated uptake pathway can be blocked by chlorpromazine, a cationic amphiphile [40]; lipid raft plays an important role in caveolin-dependent endocytosis pathway and nystatin can strongly inhibit this pathway via blocking the lipid raft; the activity of dynamin in clathrin-mediated and caveolin-dependent pathway can be noncompetitively inhibited by dynasore [41]. It can be seen in Fig. 2g that the relative cellular uptake of polyplexes is significantly reduced (∼25%) after the cells were treated with chlorpromazine, suggesting that the internalization of two polyplexes is related to clathrin-dependent uptake pathway. In contrast, the nystatin treatment group does not seem to result in any reduction of the cellular uptake of polyplexes, revealing that the polyplexes are taken up by the caveolin-dependent endocytosis pathway. Meanwhile, the treatment of dynasore also causes a significant decrease in the cellular uptake of the polyplexes, likely due to the inhibition of clathrin-mediated endocytic pathway. There are almost no differences between FBS-containing and FBS-free groups and between Mor-modified and Mor-free groups. These results indicate that the modification of CBAA and/or Mor does not impact the cellular uptake pathway of the dendrimer-based gene delivery system, in agreement with the literature [42].

3.7. Intracellular trafficking and localization of the polyplexes

The modification of dendrimer surface may influence their biological property, resulting in changes of intracellular distribution and localization [43,44]. To check the intracellular uptake of the vector/pDNA polyplexes, Cy3-labeled pEGFP DNA was further used to explore the intracellular distribution and endosomal escape of the polyplexes in HeLa cells. After 2 h, 4 h, 8 h or 12 h transfection with different vector/pDNA polyplexes, HeLa cells were stained with Lysotracker green (green) for lysosome and DAPI for nuclei (blue), respectively. As shown in Fig. 4, there are nearly no difference between groups transfected in FBS-free or 10% FBS-containing medium under the same transfection conditions. After 2 h transfection, CBAA-modified polyplexes can be uptaken by cells, but only a small portion of them enters the lysosome except the Mor-modified polyplexes. Some reports in the literature have shown that after cellular uptake, the polyplexes are usually entrapped within the early endosomes and are fused with acidic lysosomes or transport back to the intercellular space [45,46]. In this study, the strong red fluorescence of cells was found even after 4 h, 8 h and 12 h transfection, indicating that the vector/pDNA polyplexes have not been affected by lysosomal enzymes. After 2 h transfection, a small part of red and green fluorescence signals is co-localized in cells treated with Mor-modified vector/pDNA polyplexes, meaning that part of the polyplexes has entered into the lysosomes. While for cells treated with Mor-free polyplexes, there is no such apparent co-localization, suggesting that the lysosome-targeting property of the {$(Au^0)_{25}$-G5.NH_2-CBAA-PEG-Mor}/pDNA polyplexes slightly increases the lyosomal uptake of the polyplexes. With the time of transfection, more polyplexes are accumulated in the lysosomes for all groups, and the peak lysosome internalization of the polyplexes occurs at 8 h. Differing from the results reported in our previous study [24] that most of the Cy3-labled polyplexes were co-localized within the lysosomes and around the nuclei after transfection for 2 h, the zwitterion CBAA-modified polyplexes entered into cells and lysosomes more slowly, likely resulting from the antifouling property (protein resistance ability) of the polyplexes rendered by CBAA modification [33].

3.8. Inhibition of cancer cell metastasis with HIC1 pDNA transfection

We next checked if the transfection of HIC1 pDNA is able to inhibit the migration and metastasis of cancer cells. After being scraped, the HeLa cells seeded in 24 wells plate were treated with the vector/HIC1 pDNA polyplexes for 3 h under different

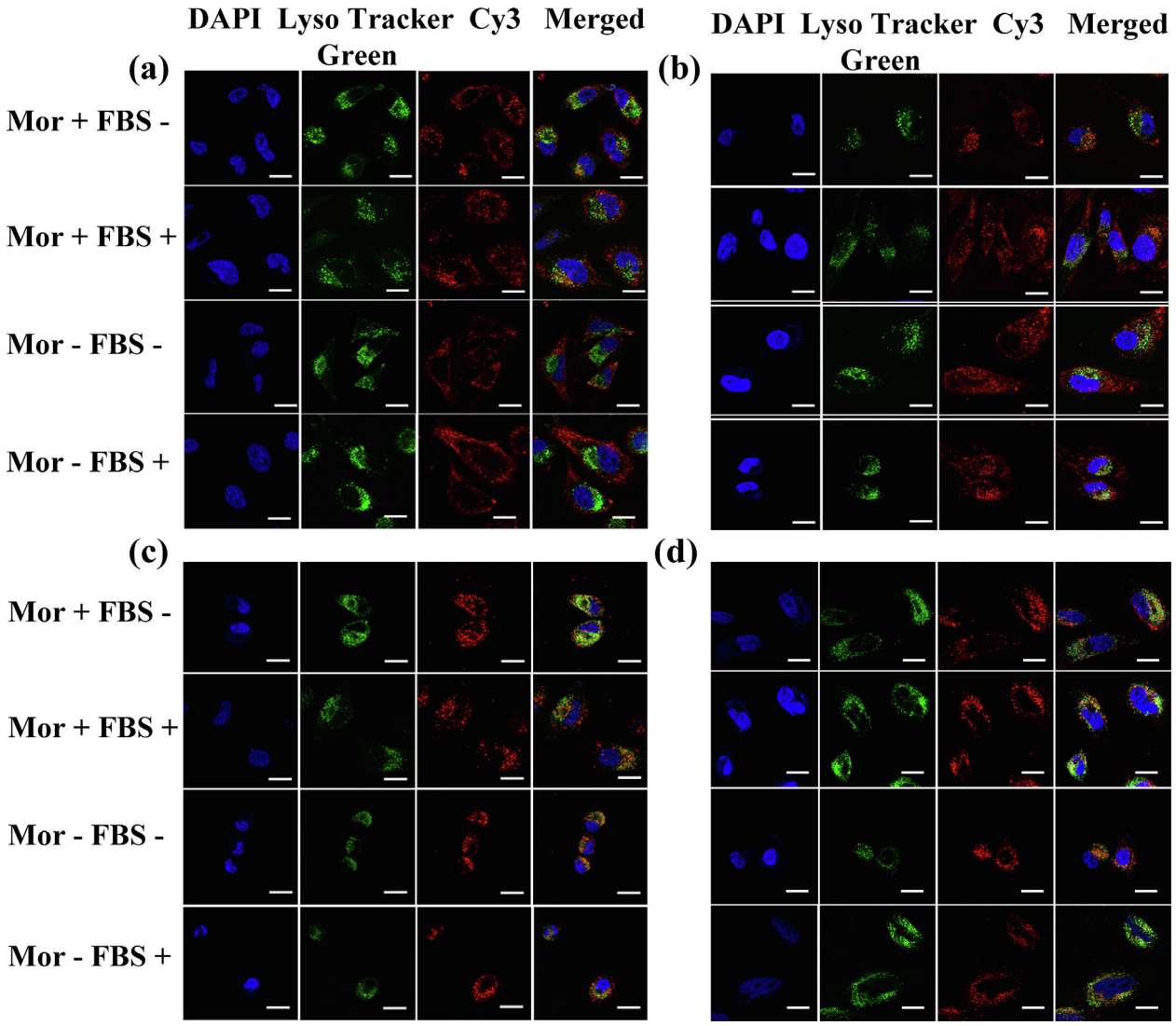

Fig. 4. Confocal microscopic images of HeLa cells incubated with different vector/pDNA polyplexes at an N/P ratio of 4:1. The cells were seeded at a density of 5×10^4 cell/well, and after cultured to confluence the cells were incubated with the respective polyplexes for 2 h (a), 4 h (b), 8 h (c) and 12 h (d), respectively.

conditions, followed by culture in fresh complete medium. The images of the wound are taken and calculated before transfection and after 12 h and 24 h transfection, respectively. As shown in Fig. 5a, for control and naked pDNA groups, the cells in-between the scraped wound gap migrate to the blank area after 12 h transfection, and at 24 h transfection, the cells significantly spread in-between the scratched gap. In contrast, all groups of cells treated with vector/HIC1 pDNA polyplexes have limited migration. The corresponding quantitative cell migration area data are shown in Fig. 5b. It can be seen that after 12 h transfection, the cell migration area for cells treated with vector/pDNA polyplexes in FBS-containing transfection environment is significantly less than that of control group ($p < 0.001$). The Mor – FBS + and Mor + FBS + groups display significantly stronger anti-migratory effect than the corresponding Mor – FBS – and Mor + FBS – groups without FBS, respectively ($p < 0.05$). After 24 h, the differences are amplified among all groups. The cell migration area of control and naked pDNA groups are up to 58.27% and 49.82%, while for Mor + FBS –, Mor + FBS +, Mor – FBS and Mor – FBS + groups, the corresponding cell migration area data approach to 36.02%, 37.04%, 28.94% and 26.69%, respectively. All groups treated with the vector/HIC1 pDNA polyplexes show significant differences from the control and naked pDNA groups ($p < 0.001$), suggesting that the cells are able to express HIC1 protein for effective inhibition of cancer cell migration [47]. It is interesting to note that there are no appreciable differences between FBS – and FBS + groups after 24 h's gene transfection in terms of the cancer cell migration, presumably due to the fact that at a later time point, the FBS-enabled nutritional factor to cells is not as significant as an earlier time point such as 12 h. Interestingly, all groups transfected with Mor-free polyplexes display much stronger anti-migratory effect than those treated with the Mor-modified polyplexes ($p < 0.05$), presumably due to the Mor-enabled lysosome targeting ability of the polyplexes that compromises their gene delivery efficiency to some extent.

Western blot assay was further conducted to demonstrate the HIC1 protein expression in cancer cells after the cells were transfected with vector/HIC1 pDNA polyplexes (Fig. 5c). The relative protein expression level of FBS + and FBS – groups hardly show differences. Apparently, HIC1 protein of cells transfected with polyplexes is significantly higher than the control and naked pDNA groups ($p < 0.01$). It seems that cells treated with Mor-free polyplexes display a higher HIC1 protein expression than those treated with the Mor-modified polyplexes. Our data suggest that cancer cells are able to be effectively transfected with HIC1 gene using the Mor-free polyplexes to inhibit their migration and metastasis.

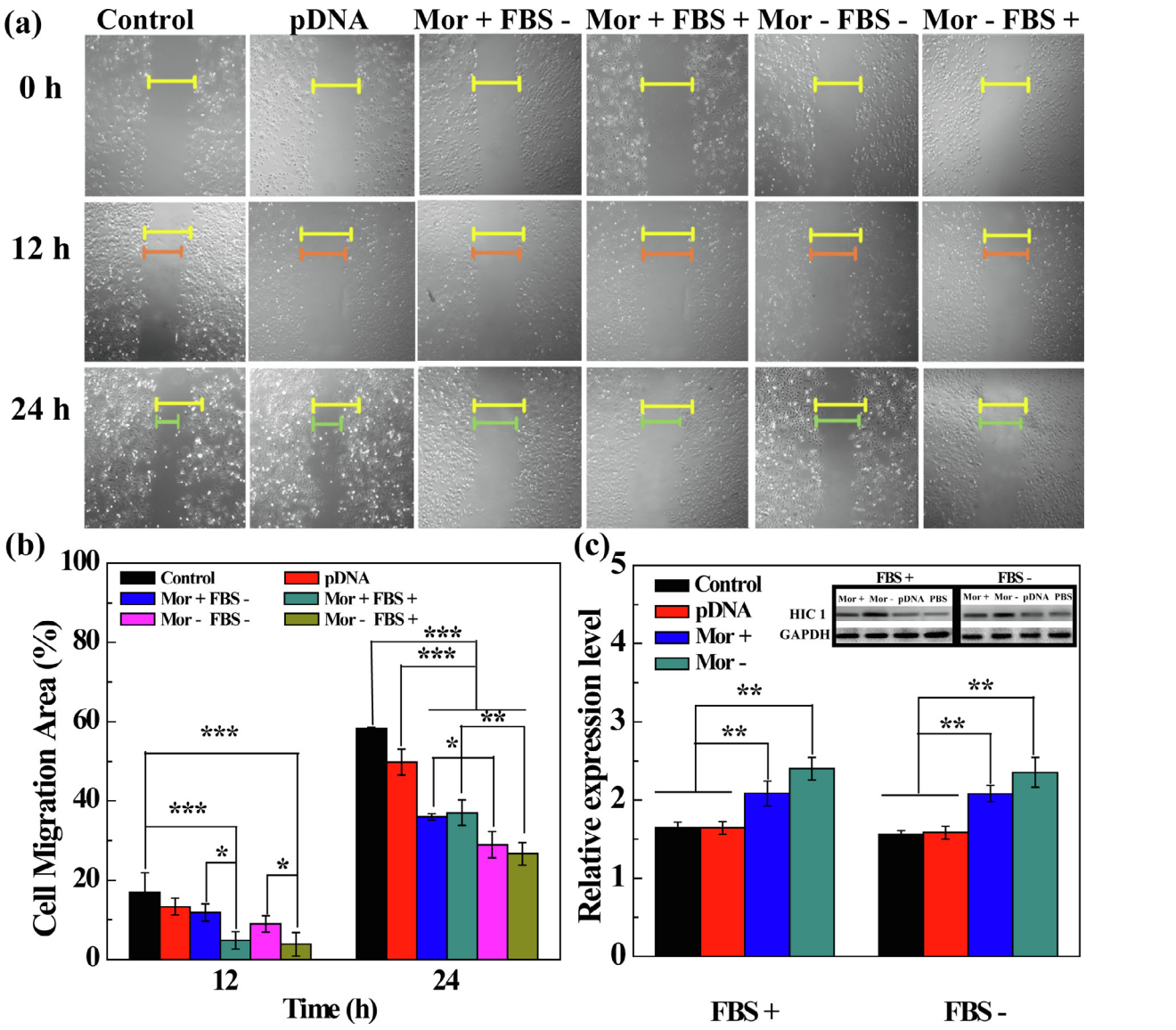

Fig. 5. Phase contrast microscopic images (a) and the corresponding cell migration area (b) of HeLa cells before and after they were transfected with vector/pDNA polyplexes for 12 and 24 h, respectively for the wound-healing assay. (c) Western blot analysis of HIC1 protein expression in HeLa cells after the cells were transfected with vector/pDNA polyplexes in FBS-free and FBS-containing medium. Inset of (c) shows the representative western blotting images of HIC1 expression. GAPDH was used as an internal control.

4. Conclusion

In summary, we have developed zwitterion CBAA-modified Au DENPs for serum-enhanced gene delivery of HIC1 gene for effective inhibition of cancer cell migration and metastasis. We show that G5 PAMAM dendrimers partially modified with CBAA can be used as templates to synthesize Au core NPs with a size of 1.5 nm. The generated Au DENPs can compact pDNA to form polyplexes with desired surface potential, hydrodynamic size, cytocompatibility, and optimal gene delivery efficiency at an N/P ratio of 4 in a serum-containing environment due to the CBAA-enabled protein resistance ability of the polyplexes. Although further modification of Mor renders the formed polyplexes with lyososome targeting ability, while the gene delivery efficiency of the polyplexes is compromised to some extent. With the demonstrated non-compromised intracellular uptake pathway and co-localization of the Mor-free polyplexes, cancer cells can be effectively transfected with HIC1 gene for expression of HIC1 protein, allowing for effective inhibition of cancer cell migration and metastasis. Through the versatile dendrimer nanotechnology, the developed vector system may be further used to load drugs [48] and be modified with targeting ligand and diagnostic agent [49] for effective combination therapy and diagnosis of different cancer types.

Acknowledgements

This research is financially supported by the National Key R&D Program (2017YFE9126200), National Natural Science Foundation of China (21773026, 81761148028 and 21911530230), the Science and Technology Commission of Shanghai Municipality (19XD1400100, 17540712000 and 18520750400), and the Fundamental Research Funds for the Central Universities (X. Shi and Z. Xiong). X. Shi also acknowledges the support by FCT-Fundação para a Ciência e a Tecnologia (project PEst-OE/QUI/UI0674/2019, CQM, Portuguese Government funds), and through Madeira 14-20 Program, project PROEQUIPRAM - Reforço do Investimento em Equipamentos e Infraestruturas Científicas na RAM (M1420-01-0145-FEDER-000008) and by ARDITI-Agência Regional para o

Desenvolvimento da Investigação Tecnologia e Inovação, through the project M1420-01-0145-FEDER-000005 - Centro de Química da Madeira - CQM$^+$ (Madeira 14-20).

Declaration of Competing Interest

The authors declare that they have no known competing financial interests or personal relationships that could have appeared to influence the work reported in this paper.

Appendix A. . Supplementary material

Detailed materials, methods and additional data of DLS, surface potential, ^{1}H NMR, antifouling property and cytotoxicity.

Appendix B. Supplementary data

Supplementary data to this article can be found online at https://doi.org/10.1016/j.actbio.2019.09.005.

References

[1] F. Chen, L. Kong, L. Wang, Y. Fan, M. Shen, X. Shi, Construction of core-shell tecto dendrimers based on supramolecular host-guest assembly for enhanced gene delivery, J. Mater. Chem. B 5 (43) (2017) 8459–8466.
[2] J. Qiu, L. Kong, X. Cao, A. Li, P. Wei, L. Wang, S. Mignani, A. Caminade, J. Majoral, X. Shi, Enhanced delivery of therapeutic siRNA into glioblastoma cells using dendrimer-entrapped gold nanoparticles conjugated with beta-cyclodextrin, Nanomaterials 8 (2018) 131.
[3] L. Kong, L. Xing, B. Zhou, L. Du, X. Shi, Dendrimer-modified MoS2 nanoflakes as a platform for combinational gene silencing and photothermal therapy of tumors, ACS Appl. Mater. Interfaces 9 (19) (2017) 15995–16005.
[4] M.M. Wales, M.A. Biel, W. Eldeiry, B.D. Nelkin, P. Issa, W.K. Cavenee, S.J. Kuerbitz, S.B. Baylin, P53 activates expression of HCI-1, a new candidate tumor-suppressor gene on 17p13.3, Nat. Med. 1 (6) (1995) 570–577.
[5] H. Eggers, S. Steffens, A. Grosshennig, J.U. Becker, J. Hennenlotter, A. Stenzl, A.S. Merseburger, M.A. Kuczyk, J. Serth, Prognostic and diagnostic relevance of hypermethylated in cancer 1 (HIC1) CpG island methylation in renal cell carcinoma, Int. J. Oncol. 40 (5) (2012) 1650–1658.
[6] Y. Chen, C. Ko, P. Lin, W. Chuang, C. Hsu, P. Chu, M. Pai, C. Chang, M. Kuo, Y. Chu, C. Tung, T.H.M. Huang, Y.W. Leu, S.H. Hsiao, Clustered DNA methylation changes in polycomb target genes in early-stage liver cancer, Biochem. Biophys. Res. Commun. 425 (2) (2012) 290–296.
[7] N. Nishida, M. Kudo, T. Nagasaka, I. Ikai, A. Goel, Characteristic patterns of altered DNA methylation predict emergence of human hepatocellular carcinoma, Hepatology 56 (3) (2012) 994–1003.
[8] G. Zhao, Q. Qin, J. Zhang, Y. Liu, S. Deng, L. Liu, B. Wang, K. Tian, C. Wang, Hypermethylation of HIC1 promoter and aberrant expression of HIC1/SIRT1 might contribute to the carcinogenesis of pancreatic cancer, Ann. Surg. Oncol. 20 (2013) S301–S311.
[9] J. Zheng, J. Wang, X. Sun, M. Hao, T. Ding, D. Xiong, X. Wang, Y. Zhu, G. Xiao, G. Cheng, M. Zhao, J. Zhang, J. Wang, HIC1 modulates prostate cancer progression by epigenetic modification, Clin. Cancer. Res. 19 (6) (2013) 1400–1410.
[10] D. Kilinc, O. Ozdemir, S. Ozdemir, E. Korgali, B. Koksal, A. Uslu, Y.E. Gultekin, Alterations in promoter methylation status of tumor suppressor HIC1, SFRP2, and DAPK1 genes in prostate carcinomas, DNA Cell Biol. 31 (5) (2012) 826–832.
[11] J. Svedlund, S.K. Edblom, V.E. Marquez, G. Akerstrom, P. Bjorklund, G. Westin, Hypermethylated in cancer 1 (HIC1), a tumor suppressor gene epigenetically deregulated in hyperparathyroid tumors by histone H3 lysine modification, J. Clin. Endocrinol. Metab. 97 (7) (2012) E1307–E1315.
[12] B.R. Rood, H.Z. Zhang, D.M. Weitman, P.H. Cogen, Hypermethylation of HIC-1 and 17p allelic loss in medulloblastoma, Cancer Res. 62 (13) (2002) 3794–3797.
[13] J. Brieger, W. Pongsapich, S.A. Mann, J. Hedrich, K. Fruth, B. Pogozelski, W.J. Mann, Demethylation treatment restores HIC1 expression and impairs aggressiveness of head and neck squamous cell carcinoma, Oral Oncol. 46 (9) (2010) 678–683.
[14] F. Farzaneh, U. Trefzer, W. Sterry, P. Walden, Gene therapy of cancer, Immunol. Today 19 (7) (1998) 294–296.
[15] C.E. Thomas, A. Ehrhardt, M.A. Kay, Progress and problems with the use of viral vectors for gene therapy, Nat. Rev. Genet. 4 (5) (2003) 346–358.
[16] P. Mancheno-Corvo, P. Martin-Duque, Viral gene therapy, viral gene therapy, Clin. Transl. Oncol. 8 (12) (2006) 858–867.
[17] M.A. Kay, J.C. Glorioso, L. Naldini, Viral vectors for gene therapy: the art of turning infectious agents into vehicles of therapeutics, Nat. Med. 7 (1) (2001) 33–40.
[18] D. Luo, W.M. Saltzman, Synthetic DNA delivery systems, Nat. Biotechnol. 18 (1) (2000) 33–37.
[19] J. Wu, D. Yamanouchi, B. Liu, C.C. Chu, Biodegradable arginine-based poly (ether ester amide)s as a non-viral DNA delivery vector and their structure-function study, J. Mater. Chem. 22 (36) (2012) 18983–18991.
[20] C.M. Paleos, L.A. Tziveleka, Z. Sideratou, D. Tsiourvas, Gene delivery using functional dendritic polymers, Expert Opin. Drug Delivery 6 (1) (2009) 27–38.
[21] T. Xiao, X. Cao, X. Shi, Dendrimer-entrapped gold nanoparticles modified with folic acid for targeted gene delivery applications, Nat. Biotechnol. 172 (1) (2013) E114–E115.
[22] L. Kong, Y. Wu, C.S. Alves, X. Shi, Efficient delivery of therapeutic siRNA into glioblastoma cells using multifunctional dendrimer-entrapped gold nanoparticles, Nanomedicine 11 (23) (2016) 3103–3115.
[23] W. Hou, P. Wei, L. Kong, R. Guo, S. Wang, X. Shi, Partially PEGylated dendrimer-entrapped gold nanoparticles: a promising nanoplatform for highly efficient DNA and siRNA delivery, J. Mater. Chem. B 4 (17) (2016) 2933–2943.
[24] Y. Shan, T. Luo, C. Peng, R. Sheng, A. Cao, X. Cao, M. Shen, R. Guo, H. Tomas, X. Shi, Gene delivery using dendrimer-entrapped gold nanoparticles as nonviral vectors, Biomaterials 33 (10) (2012) 3025–3035.
[25] L. Kong, C.S. Alves, W. Hou, J. Qiu, H. Moehwald, H. Tomas, X. Shi, RGD peptide-modified dendrimer-entrapped gold nanoparticles enable highly efficient and specific gene delivery to stem cells, ACS Appl. Mater. Interfaces 7 (8) (2015) 4833–4843.
[26] T. Zhang, Y. Huang, X. Ma, N. Gong, X. Liu, L. Liu, X. Ye, B. Hu, C. Li, J. Tian, A. Magrini, J. Zhang, W. Guo, J. Xing, M. Bottini, X. Liang, Fluorinated oligoethylenimine nanoassemblies for efficient siRNA-mediated gene silencing in serum-containing media by effective endosomal escape, Nano Lett. 18 (10) (2018) 6301–6311.
[27] M. Ogris, S. Brunner, S. Schuller, R. Kircheis, E. Wagner, PEGylated DNA/transferrin-PEI complexes: reduced interaction with blood components, extended circulation in blood and potential for systemic gene delivery, Gene Ther. 6 (4) (1999) 595–605.
[28] M.R. Rekha, C.P. Sharma, Blood compatibility and in vitro transfection studies on cationically modified pullulan for liver cell targeted gene delivery, Biomaterials 30 (34) (2009) 6655–6664.
[29] D. Kim, S. Park, J.H. Lee, Y.Y. Jeong, S. Jon, Antibiofouling polymer-coated gold nanoparticles as a contrast agent for in vivo x-ray computed tomography imaging, J. Am. Chem. Soc. 129 (24) (2007) 7661–7665.
[30] D. Ma, J. Chen, Y. Luo, H. Wang, X. Shi, Zwitterion-coated ultrasmall iron oxide nanoparticles for enhanced T-1-weighted magnetic resonance imaging applications, J. Mater. Chem. B 5 (35) (2017) 7267–7273.
[31] P. Wang, J. Yang, B. Zhou, Y. Hu, L. Xing, F. Xu, M. Shen, G. Zhang, X. Shi, Antifouling manganese oxide nanoparticles: synthesis, characterization, and applications for enhanced MR imaging of tumors, ACS Appl. Mater. Interfaces 9 (1) (2017) 47–53.
[32] L. Wang, Z. Wang, G. Ma, W. Lin, S. Chen, Reducing the cytotoxity of poly (amidoamine) dendrimers by modification of a single layer of carboxybetaine, Langmuir 29 (28) (2013) 8914–8921.
[33] Z. Xiong, Y. Wang, J. Zhu, X. Li, Y. He, J. Qu, M. Shen, J. Xia, X. Shi, Dendrimers meet zwitterions: development of a unique antifouling nanoplatform forenhanced blood pool, lymph node and tumor CT imaging, Nanoscale 9 (34) (2017) 12295–12301.
[34] H. Yu, Y. Xiao, L. Jin, A lysosome-targetable and two-photon fluorescent probe for monitoring endogenous and exogenous nitric oxide in living cells, J. Am. Chem. Soc. 134 (42) (2012) 17486–17489.
[35] S. Ashraf, J. Park, M.A. Bichelberger, K. Kantner, R. Hartmann, P. Maffre, A.H. Said, N. Feliu, J. Lee, D. Lee, G.U. Nienhaus, S. Kim, W.J. Parak, Zwitterionic surface coating of quantum dots reduces protein adsorption and cellular uptake, Nanoscale 8 (41) (2016) 17794–17800.
[36] J. Qiu, L. Kong, X. Cao, A. Li, H. Tan, X. Shi, Dendrimer-entrapped gold nanoparticles modified with beta-cyclodextrin for enhanced gene delivery applications, RSC Adv. 6 (31) (2016) 25633–25640.
[37] S.D. Conner, S.L. Schmid, Regulated portals of entry into the cell, Nature 422 (6927) (2003) 37–44.
[38] H. Lee, H. Mok, S. Lee, Y. Oh, T.G. Park, Target-specific intracellular delivery of siRNA using degradable hyaluronic acid nanogels, J. Controlled Release 119 (2) (2007) 245–252.
[39] T.G. Park, J.H. Jeong, S.W. Kim, Current status of polymeric gene delivery systems, Adv. Drug Delivery Rev. 58 (4) (2006) 467–486.
[40] T.G. Iversen, T. Skotland, K. Sandvig, Endocytosis and intracellular transport of nanoparticles: present knowledge and need for future studies, Nano Today 6 (2) (2011) 176–185.
[41] S. Peng, C. Su, M. Wei, C. Chen, Z. Liao, P. Lee, H. Chen, H. Sung, Effects of the nanostructure of dendrimer/DNA complexes on their endocytosis and gene expression, Biomaterials 31 (21) (2010) 5660–5670.
[42] A. Li, J. Qiu, B. Zhou, B. Xu, Z. Xiong, X. Hao, X. Shi, X. Cao, The gene transfection and endocytic uptake pathways mediated by PEGylated PEI-entrapped gold nanoparticles, Arabian J. Chem. (2019), https://doi.org/10.1016/j.arabjc.2018.06.009.
[43] R. Jevprasesphant, J. Penny, D. Attwood, N.B. McKeown, A. D'Emanuele, Engineering of dendrimer surfaces to enhance transepithelial transport and reduce cytotoxicity, Pharm. Res. 20 (10) (2003) 1543–1550.
[44] K.M. Kitchens, R.B. Kolhatkar, P.W. Swaan, N.D. Eddington, H. Ghandehari, Transport of poly(amidoamine) dendrimers across caco-2 cell monolayers: influence of size, charge and fluorescent labeling, Pharm. Res. 23 (12) (2006) 2818–2826.

[45] I.A. Khalil, K. Kogure, H. Akita, H. Harashima, Uptake pathways and subsequent intracellular trafficking in nonviral gene delivery, Pharmacol. Rev. 58 (1) (2006) 32–45.
[46] H.Y. Nam, S.M. Kwon, H. Chung, S. Lee, S. Kwon, H. Jeon, Y. Kim, J.H. Park, J. Kim, S. Her, Y.K. Oh, I.C. Kwon, K. Kim, S.Y. Jeong, Cellular uptake mechanism and intracellular fate of hydrophobically modified glycol chitosan nanoparticles, J. Controlled Release 135 (3) (2009) 259–267.
[47] P. Li, X. Liu, Z. Dong, Z. Ling, Epigenetic silencing of HIC1 promotes epithelial-mesenchymal transition and drives progression in esophageal squamous cell carcinoma, Oncotarget 6 (35) (2015) 38151–38165.
[48] H. Xiang, Q. Deng, L. An, M. Guo, S. Yang, J. Liu, Tumor cell specific and lysosome-targeted delivery of nitric oxide for enhanced photodynamic therapy triggered by 808 nm near-infrared light, Chem. Commun. 52 (1) (2016) 148–151.
[49] S. Wen, K. Li, H. Cai, Q. Chen, M. Shen, Y. Huang, C. Peng, W. Hou, M. Zhu, G. Zhang, X. Shi, Multifunctional dendrimer-entrapped gold nanoparticles for dual mode CT/MR imaging applications, Biomaterials 34 (5) (2013) 1570–1580.